NIBS 2020 Reference Sheets

T. Sarmento[1,a)], D. Wünderlich[2], U. Fantz[2,3], R. Friedl[3], D. Rauner[3], K. Tsumori[4], L. Shenjin[5], W. Chen[5], D. Bollinger[6], O. Hidetomo[7], K. Shinto[7], I. Draganic[8], R. F. Welton[9]

[1] STFC ISIS Pulsed Spallation Neutron and Muon Facility, Rutherford Appleton Laboratory, OX11 0QX Harwell, United Kingdom
[2]Max-Planck-Institut für Plasmaphysik, Boltzmannstr. 2, 85748 Garching, Germany
[3]AG Experimentelle Plasmaphysik, Universität Augsburg, 86135 Augsburg, Germany
[4]National Institute for Fusion Science, Oroshi, Toki, Gifu 509-5292, Japan
[5]China Spallation Neutron Source (CSNS), Institute of High Energy Physics (IHEP), Chinese Academy of Sciences (CAS), 523803 Dongguan, China
[6]Fermi National Accelerator Laboratory, Box 500, Batavia, IL 60510, USA
[7]J-PARC Center, Tokai-mura, Naka-gun, Ibaraki-ken 319-1195, Japan
[8]Los Alamos National Laboratory, Los Alamos, NM 87545, USA
[9]Spallation Neutron Source, Oak Ridge National Laboratory, Oak Ridge, USA

[a)]Corresponding author: tiago.sarmento@stfc.ac.uk

Abstract. In preparation for NIBS 2020 various labs prepared reference sheets containing key information about their ion sources and the machines that they serve. The contents of the reference sheets have been formatted and edited into this paper for posterity and ease of access.

INTRODUCTION

The 2020 Negative Ion Beams Symposium (NIBS) was hosted online, accessible for free and live in various time zones as a joint venture between national laboratories. A higher number of newcomers compared to previous conferences was expected. In order to welcome those less familiar with negative ion beams and sources, and also to refresh the memories of experienced attendees, an introductory series of tutorials were presented and laboratories were invited to submit a reference sheet for the audience to use during and after the symposium.

The reference sheets were designed to contain key ion source and laboratory details. A reminder of laboratories' equipment, research, and motivation, proved popular even among regular attendees. This paper contains the information in the reference sheets that were submitted, formatted to publish in the proceedings for posterity and easy access. Note that although many key laboratories are represented, this is by no means a complete list of ion source research facilities. Furthermore, the physics of ion sources are not explained or explored in this text, but may be found in [1-3].

The sources separated into fusion and accelerator sources are listed here:

Fusion regular operational sources

- National Institute for Fusion Science (NIFS)

Fusion sources under development

- ITER
- IPP Garching
- Small fusion test stands

Accelerator regular operational sources:

- Chinese Spallation Neutron Source (CSNS)
- Fermilab
- ISIS Neutron and Muon Source
- Japan – Proton Accelerator Research Complex (J-PARC)
- Los Alamos Neutron Science Centre (LANSCE)
- Spallation Neutron Source (SNS)

FUSION SOURCES

The development of fusion power is a globally coordinated effort with a long range roadmap of international projects and national laboratories from JET, JT60, LHD, ITER to DEMO.

Fusion machines require high power neutral beams to heat and current drive the fusion plasma. The beam must be charge neutral to allow it to be injected through the strong magnetic fields used to confine the fusion plasma. Neutral beams are produced by accelerating a charged ion beam then converting it to a neutral beam. For high energy (1 MeV) beams the efficiency of this neutralisation process dictates the usage of negative ions. The largest fusion machines currently operating negative ion beam based neutral beam injectors are the JT60 and the LHD machines in Japan. ITER injectors are still several years away from operation.

There are ITER test stands of various scales for negative ion based neutral beam injectors in Germany and Italy.

National Institute for Fusion Sources (NIFS)

Negative-ion-based negative beam injectors (N-NBIs) have been developed from 1980s and utilized for plasma heating and current drive at QST (National Institute for Quantum and Radiological Science and Technology) and NIFS (National Institute for Fusion Science) since the 1990s [4-6]. To obtain a uniform beam over a wide area aiming at homogeneous NB injection, filament-arc source technology, which had been sufficiently established in positive ion NBI, was adopted for negative ion source development at QST and NIFS. The NIFS ion source is a multi-cusp source equipped with a pair of large parallel permanent magnets called “filter magnets” inducing a ~0.6 mT transversal magnetic field at the centre in the direction of the short side of the ion source, or the direction parallel to the plasma grid (PG). The filter magnetic field reduces the energy of electrons generated by the filament arc discharge cathode, biased at about -80V in the “driver region”, down to less than 1 eV in the “beam extraction region” in front of the PG. Produced negative ions near the PG are extracted without being destroyed by the electron collisional detachment because of sufficiently low electron energy. The short side dimension of the plasma chamber is as small as 350 mm, and the uniformity of the filter magnetic field is adjusted by arranging the spatial intervals of the filter magnets. Negative ion yield is enhanced by continuously injecting caesium (Cs) vapour at a small flow rate during source operation.

Two types of NBI beamlines are installed at NIFS; one is a NBI test stand and the others are actual injectors to heat the plasmas confined in the Large Helical Device (LHD). The former beamline has been applied for the research and development to construct LHD NBI and later it has been utilized to improve the performance of NBI ion sources. In the recent decade, the test-stand beamline has been used to study the source plasma and beam characteristics. Top and side views of the test-stand are illustrated in Figure 1.

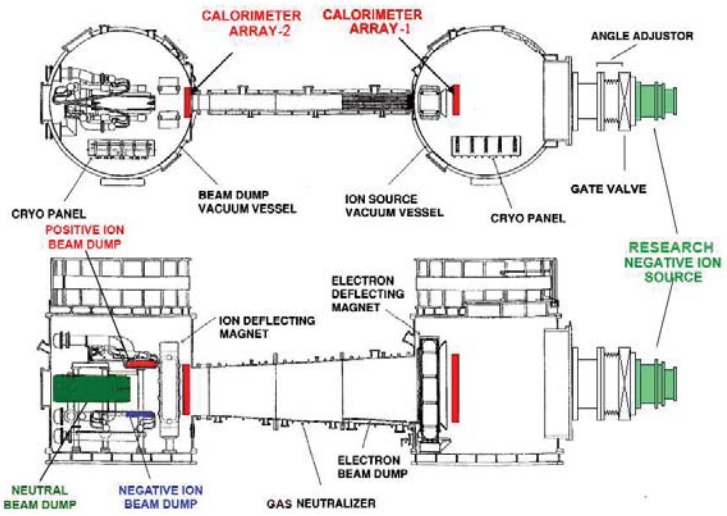

FIGURE 1. Top (upper) and side (lower) views of NIFS NBI test stand.

The test-stand beamline is designed nearly identical to the LHD NBI beamlines and is equipped with a full set of peripheral devices, including cryo-sorption pumps, a gas neutralizer, ion and neutral beam dumps. Negative ion current is evaluated from an integrated heat flux with two cross-shaped movable calorimeter arrays installed at the entrance and exit of the neutralizer. An ion source with internal dimensions, 700 mm (H) x 350 mm (W) x 230 mm (D), half the length of the LHD source, is normally installed on the test-stand. Two segments of single-staged accelerator consisting of PG, Extraction Grid (EG), Steering Grid (SG) and Grounded Grid (GG) are installed in the source and two Cs feeding lines are equipped at the backplate via diffuser nozzles injecting the Cs vapour to the internal sidewalls. A short side cross-sectional view of the ion source called "Research-and-development Negative Ion Source (RNIS)" is shown in Figure 2(a). Various plasma diagnostic modules are installed on the bias insulator as indicated in Figure 2(b). These diagnostic modules are utilized to study how the plasma characteristics in the extraction region affect the extracted negative ion beam quality. In the extraction region, magnetic field intensity and the direction change 3-dimensionally depending on the distance from the PG surface, and most of the diagnostic modules are movable in 3 orthogonal directions. The development of some diagnostic systems, like cavity ringdown measurement, is supported by IPP Garching [7].

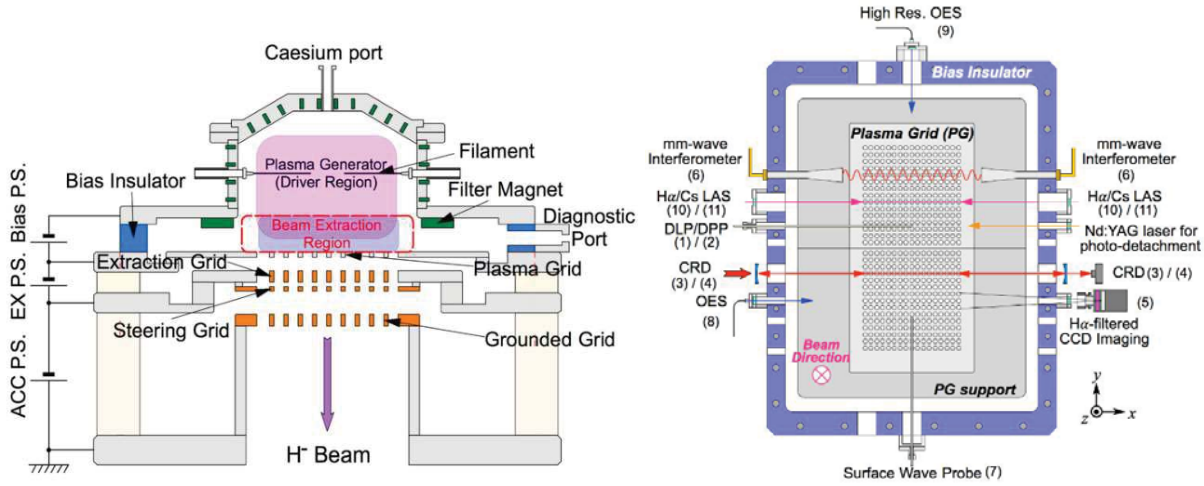

FIGURE 2. A short-side view of the NIFS RNIS (left) and the arrangement of the diagnostic modules short-side view of the NIFS RNIS (right).

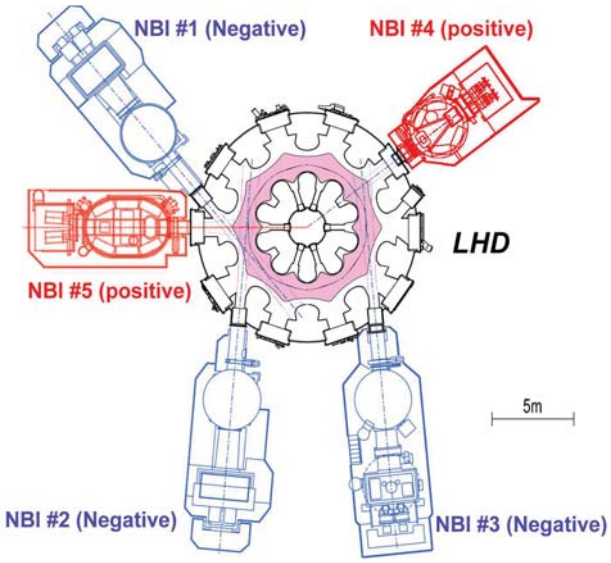

FIGURE 3. Schematic views of LHD NBI system.

In order to investigate meniscus formation of the plasma in the negative ion source, beam/beamlet diagnostics projects have started. A beamlet monitor, Mini STRIKE made of one-directional CFC tile, has been introduced from Consorzio RFX to NIFS NBI test stand [8], and a wider beamlet monitor was built at NIFS. Concerning the beamlet characteristics, phase space analyses combined with the pepper-pot emittance meter [9] and simulation study have been carried out [10].

The results obtained at NIFS NBI test stand were utilized to improve the performance of the negative-ion-based NBI system for LHD. A schematic view of the LHD NBI system is shown in Figure 3. Two ion sources of inner

TABLE 1. Parameters of LHD N-NBI source and RNIS

	N-NBI source	RNIS
Arc Power [kW] （Specification）	300 kW (maximum)	300 kW (maximum)
Source Size [mm]	NBI#1: 1400(H) x 350(W) x 230(D) NBI#2&3: 1400(H) x 350(W) x 220(D)	700(H) x 350(W) x 230(D)
Extraction Area [mm^2]	1250(H) x 250(W)	500(H) x 250(W)
Number of Apertures	NBI#1: 960 = 5 seg. x 16(H) x 12(V) NBI#2&3: 840 = 5 seg. x 14(H) x 12(V)	360 = 2 seg. x 15(H) x12(V)
Aperture size [mm]	NBI#1: ϕ 12 NBI#2&3: ϕ 14	ϕ 11
Accelerated Current [A] (specification)	90 (power supply maximum)	90 (power supply maximum)
Beam energy [keV]	190 (maximum)	95 (maximum)
Number of Cs line	3 lines	2 lines

dimensions1400 mm (H) x 350 mm (W) x 220 / 230 mm (D) are installed at each negative-ion-based NBI and three Cs feeding lines are installed to every ion source. The accelerator consists of 5 segments along the direction of the beam and the Multi-Slot Grounded Grid (MSGG) is installed to all the beamlines as well as RNIS [11]. The beamlines are dedicated to stable and high-power beam injection and no extra diagnostic ports are added to the systems. The monitored source operation parameters include the discharge power input to the plasma chamber, the drain currents flowing the extraction and acceleration power supplies. Beam profiles are measured at calorimeter array in the beamline and the tile facing the inner wall of LHD. In addition, ports for Optical Emission Spectroscopy (OES) and Beam Emission Spectroscopy (BES) are installed. The beam injection power (port-through power) is recorded as the most important parameter. So far, the maximum injection power per beamline is 6.8 MW at the beam energy of 189 keV [12] with the current density as large as 370 A/m^2. Total maximum injection power for the three negative-ion-based NBIs in operation at the same time reached 16 MW [13]. Parameters of negative-ion-based NBI for LHD and RNIS are indicated in Table 1. There are two parameters in the LHD source because the source design for beamline 1 is different from that for beamlines 2 and 3.

ITER

The international fusion experiment ITER [14] will be equipped with two powerful neutral beam injection (NBI) beamlines for heating and current drive with the option to add a third one in a later stage [15]. A diagnostic injector with low power will be required to diagnose the He ash content using charge exchange resonance spectroscopy [16]. These NBI systems are based on the generation of negative hydrogen ions in a caesiated RF-driven ion source, electrostatic acceleration, and neutralisation in a hydrogen gas target. Fusion sources are much larger than accelerator sources, and have a series of electrically biased grids to extract beam and handle co-extracted electrons.

The particles shall have an energy of 870 keV and 1 MeV for hydrogen and deuterium, respectively, for the heating beams (HNB) of power up to 16.5 MW, whereas only hydrogen at 100 keV is foreseen for the diagnostic beam (DNB) of power up to 2.2 MW. The ion sources need to operate at a pressure of 0.3 Pa or below to keep the stripping losses in the 7-stage accelerator system below 30%.

The HNB's large ion source (0.9 m×1.9 m) is required to produce 57 A for 3600 s in deuterium operation and 66 A for 1000 s in hydrogen, corresponding to current densities of 286 A/m^2 and 329 A/m^2, respectively. The DNB specification is 77 A in hydrogen (391 A/m^2) at a 3 s on / 20 s off time at the repetition rate of 5 Hz. The inevitable co-extracted electrons are deflected by embedded magnets onto the second grid of the extraction system. To avoid damaging it, electron current must be lower than ion current. The homogeneity of the accelerated beam, composed of 1280 beamlets, has to be better than 90% with a core divergence of each beamlet of less than 7 mrad to ensure proper beam transport.

The requirements for the operational parameters of ion source and accelerator are very challenging and by far exceed those of the NBI systems based on negative ions (NNBI) at existing fusion devices JT-60U [4], JT-60SA [5] and LHD [6]. The ion sources at those systems are based on filament discharges (arc discharge) and are typically operating for few seconds at their nominal heating power. For reduced power, pulses up to several tens of seconds have been demonstrated. In preparation for the NBI system of JT-60SA, pulses of up to 60 s have been obtained with an accelerated current density of 190 A/m^2, but only for a small extraction area (nine apertures) [17]. For the ITER-relevant RF sources, the required ion current densities have been demonstrated at smaller test facilities [18] for a beam duration of a few seconds. Development is ongoing to satisfy ITER specifications in a worldwide collaboration.

IPP Garching

The RF-driven prototype ion source developed at IPP Garching was chosen as the reference source for the ITER NBI system in 2006. The prototype source has a size of about 0.3 m×0.6 m, and is based on plasma generation by inductive coupling (f = 1 MHz, up to 100 kW) into a cylindrical RF driver with a volume of several litres. The design is modular and it is scaled up to the ITER NBI ion source using eight drivers, feeding the plasma into one large expansion chamber (0.9 m×1.9 m).

Two test facilities are in operation at IPP Garching: BATMAN Upgrade (total extraction area: ≈ 0.01 m^2), using the prototype source, and ELISE, operating with a source of half the ITER size (0.9 m×1.0 m, four drivers, total extraction area: ≈ 0.1 m^2). A detailed overview of the work performed at IPP can be found in [19,20]. Both test facilities can be operated in hydrogen and in deuterium to demonstrate the source parameters in both ITER NBI operation regimes. The ITER parameters could be demonstrated in hydrogen, more than 90% of the required extracted

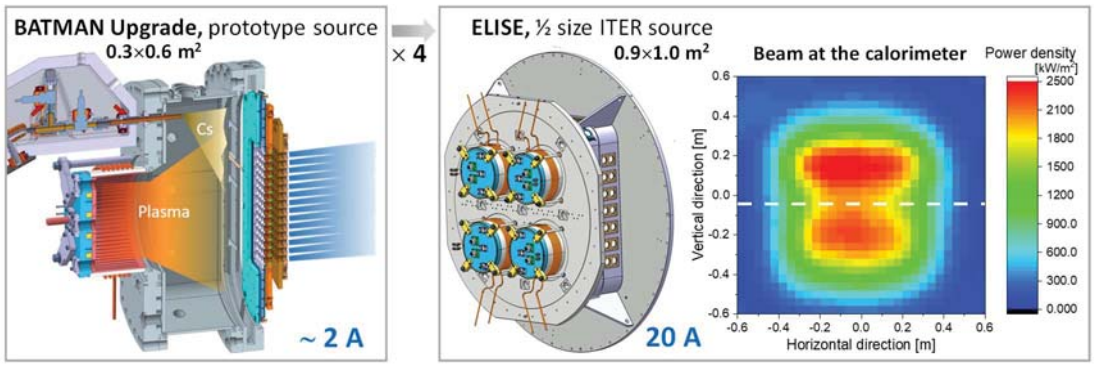

FIGURE 4. A diagram of the RF-driven ion sources at BATMAN Upgrade and at ELISE. Additionally shown is the footprint of the beam on the diagnostic calorimeter, diagnosed by IR calorimetry.

ion current for 1000 s was achieved, limited only by technical constrains regarding the available RF power and the HV power supply [21]. The achievement of the parameters in deuterium for long pulses is still pending as the co-extracted electrons are limiting the ion source performance: the amount of the co-extracted electrons, their dynamics in long pulses and their inhomogeneity in vertical direction is significantly stronger in deuterium than in hydrogen.

Figure 4 shows the prototype source and the ELISE source. An example of the beam extracted from ELISE, diagnosed by IR calorimetry, is given on the right part of the figure. Table 2 compares the design values of BATMAN Upgrade and ELISE with the ones of the ITER source. Some acronyms commonly used related to the NNBI research at IPP Garching are defined in Table 3.

In both test facilities, a horizontal magnetic filter field of a few millitesla, sufficient to magnetize electrons but not ions, is used to reduce the electron temperature and co-extracted electron current. Production of negative ions happens mainly on the caesiated Plasma Grid (PG). For the evaporation of caesium, one (BATMAN Upgrade) or two (ELISE) caesium ovens are used. Extraction and acceleration of the negative ions from the source takes place via a three-grid, multi-aperture extraction system, consisting of the PG, the extraction grid (EG) and the grounded grid (GG). The grid system of BATMAN Upgrade has 70 apertures, the one of ELISE 640 apertures, arranged in 8 aperture groups. In

TABLE 2. A comparison of BATMAN and ELISE design values with the requirements for ITER

	BATMAN Upgrade	**ELISE**	**ITER (specifications)**
RF Power	100 kW	300 kW	800 kW
Source Size	0.3 x 0.6 m^2	0.9 x 1.0 m^2	1.0 x 2.0 m^2
Extraction Area	0.01 m^2	0.1 m^2	0.2 m^2
Number of Apertures	70	640	1280
Accelerated Current	2 A	20 A	40 A
Total Voltage	50 kV	60 kV	1 MeV

TABLE 3. Acronyms commonly used related to the NNBI research at IPP Garching.

NBI	Neutral beam injection	P_{RF}	RF generator power
A_{source}	Source area	$A_{extract.}$	Extraction area
I_{acc}, U_{tot}	Accelerated current, total voltage	#apert.	Number of (extraction) apertures
PG, EG; GG	Plasma grid, extraction grid, grounded grid (source on high potential)	TDLAS	Tuneable diode laser absorption spectroscopy
OES	Optical emission spectroscopy	CRDS	Cavity ringdown spectroscopy
BES	Beam emission spectroscopy		

both experiments, the aperture diameter is 14 mm. In 2.2 m (BATMAN Upgrade) or 3.5 m (ELISE) distance to the extraction system, the negative ion beam hits a diagnostic calorimeter.

TABLE 4. Overview of the diagnostic techniques and models applied at IPP Garching. Definitions of abbreviations in Table 3.

Source diagnostics	OES	n_e, T_e, T_{gas}, T_H
	Langmuir probes	n_e, T_e, electron energy distribution function
	TDLAS	Caesium density
	CRDS	Negative ion density
Beam diagnostics	Electrical current measurements	Extracted H^- current, co-extracted e^- current
	BES	Beam uniformity and divergence, H^- stripping
	CFC tile calorimeter	Properties of single beamlets
	Beam calorimeter	Power density and its uniformity, divergence
Modelling	Fluid code	RF coupling, plasma transport
	Collisional radiative model Yacora	Plasma emission (needed for OES evaluation)
	PIC code ONIX	Plasma properties close to meniscus
	Particle tracking codes IBSimu, BBCNI, ABC3D	Beamlet properties and beam transport

Small Test Stands

University of Augsburg

Fundamental investigations supporting the ion source development at IPP Garching are performed at the University of Augsburg. The AG Experimentelle Plasmaphysik (EPP) focusses on fundamental plasma physics and diagnostics of low-temperature plasmas, in particular containing molecules. Diagnostic methods are developed for accessing general plasma parameters as well as for dedicated applications on ion sources such as the. surface ionization detector (SID) for Cs, tunable diode laser absorption spectroscopy (TDLAS), or determination of RF power transfer efficiency.

Experimental studies are accompanied by modelling for evaluation and interpretation of measurements (e.g. collisional radiative modelling, or molecular band simulation). The close intermeshing with the investigations at IPP gives valueable inputs for both sides. While the flexible experimental set ups at AG EPP can tackle specific issues of the complex ion source research with great detail, ion source operation at IPP demonstrates the scalability of fundamental results for high powers and large dimensions.

Major work focusses on the Cs dynamics on a fundamental level, in particular regarding systematic investigations on the work function of caesiated materials under ion source conditions as well as the search for Cs-free alternative materials. Furthermore, the isotopic differences between hydrogen and deuterium plasmas are investigated and first proof-of-principle studies for alternative RF concepts (planar ICPs, Helicon) and laser neutralization of negative ion beams are conducted. These core topics of investigation are highlighted in Figure 5.

To assess the specific issues of ion source research, several small-scale experiments are available in the laboratories, each of them operable with hydrogen and deuterium. Numbers and facts of the experimental set ups are given in Table 5 including the applied diagnostics. The abbreviations are explained in Table 6.

For further reading, use references [25,26] for studies related to the work function of caesiated surfaces, [27,28] for those related to caesium-free alternatives, [29,30] for investigations regarding the RF power transfer efficiency, [31] for the development of the laser neutraliser cavity, and [32] for an exemple of plasma diagnostics development, i.e. the application of an AC-driven Langmuir probe to measure the electron energy distribution function (EEDF).

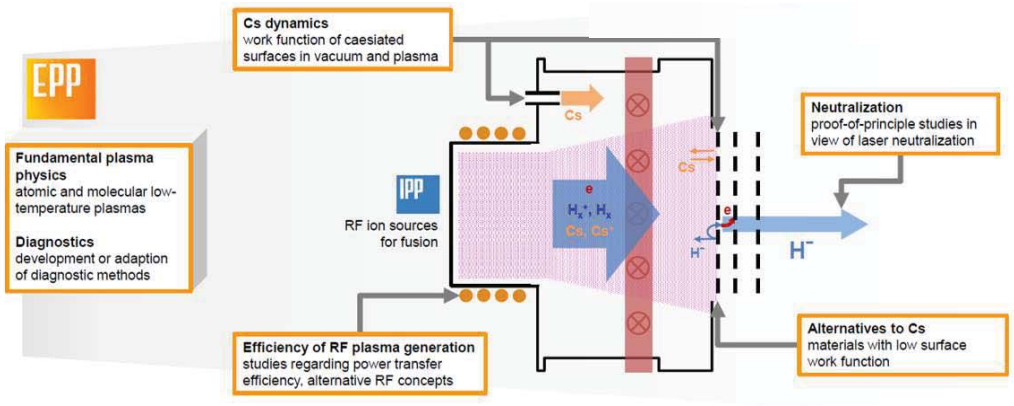

FIGURE 5. Scheme of a fusion source with the various topics studied at AG EPP, University of Augsburg.

TABLE 5. Comparison of the various experimental set ups to investigate fundamental processes relevant to fusion ion sources at AG EPP, University of Augsburg.

	ACCesS	**HOMER**	**CHARLIE**	**PlanICE**	**Laser Neutralizer Cavity**
Discharge Type	Planar ICP (27.12 MHz)	ECR (2.45 GHz)	ICP, Helicon (1-30 MHz)	Planar ICP (2 MHz)	-
Max Power	600 W	1 kW	2 kW	2 kW	8 W
Pressure Range	2 – 20 Pa	0.3 – 10 Pa	0.2 – 10 Pa	1 – 10 Pa	Cavity: < 1 mbar – 1 bar
Purpose in view of NNBI sources	Studies on caesiated surfaces, work function of Cs alternatives	Cs alternatives, low power extraction system	RF power transfer efficiency, Helicon concepts	RF power transfer efficiency	Stable coupling of cw laser into high-finesse cavity
Sample holder	Yes	Yes	No	No	-
Diagnostics	OES, Langmuir probe, WABS, TDLAS Cs, CRDS, SID, QMB, RGA, WF	OES, Langmuir probe, laser photo detachment, CRDS	OES, probes (Langmuir / double / Mach), TDLAS H_α, VUV	OES, Langmuir probe, AC probe, TDLAS H_α, VUV, EMS	Power meters, photodiode, CMOS camera, beam profiler
Modelling	CR modelling (Yacora), molecular band simulations				-

TABLE 6. Defining common acronyms used in Table 5 as well as in talks and papers by AG EPP.

ICP	inductively coupled plasma	SID	surface ionization detector
ECR	electron cyclotron resonance heating	QMB	quartz micro balance
OES	optical emission spectroscopy	RGA	residual gas analyzer
WABS	white light absorption spectroscopy	WF	work function measurement system
TDLAS	tuneable diode laser absorption spectroscopy	VUV	VUV spectroscopy
CRDS	cavity ring-down spectroscopy	EMS	energy resolved mass spectrometer
CR	collisional-radiative		

Other Test Stands

While the test facilities at IPP Garching, BATMAN Upgrade and ELISE, use smaller ion sources for developing operational scenarios and investigating basic physical effects, the ion source for ITER NBI will be commissioned and operated first at the European Neutral Beam Test Facility (NBTF) in Padua, Italy. The NBTF hosts the test facility SPIDER for the ITER NBI ion source which went into operation in 2018 and the test facility MITICA for the full ITER HNB beamline which is currently planned to go into operation in 2024. ITER-India is responsible for the DNB and is currently operating an 1/8 ITER prototype source at the test facility ROBIN, which went into operation in 2011, and an intermediate step using a ¼ ITER source – the Twin source. Finally, a full prototype DNB is under preparation including the long transmission line to the fusion device.

Accompanying programmes for the ion source and the accelerator technology are undertaken at NIFS and at QST in Japan together with support activities at Universities around the world. As an intermediate step between ITER and a commercial power plant, activities started in several countries to design a DEMO (DEMOnstration) reactor. More detailed information about the activities on negative ion sources in general and on fusion are compiled in the 2018 issue of NJP named "Focus on sources of negatively charged ions" [3].

Some other laboratories active in fusion ion source development include:

- Joint European Tokamak (JET) located in the UK, precursor to ITER, uses the SNIF ion source [33]
- Budker Institute of Nuclear Physics (BINP) in Russia has test stands contributing to N-NBI development [34].
- Doshisha University's Plasma Physics Laboratory in Japan studies fundamentals of plasmas relevant to fusion ion sources.[35]

Though there are others not covered in this paper.

ACCELERATOR SOURCES

H^- ion sources are used in accelerator facilities with synchrotron, cyclotron, or tandem accelerators. The advantages of H^- arise when the two electrons are stripped away to create a beam of protons, thus allowing the charge state of the beam to be swapped from -1 to +1.

In a synchrotron (or storage ring) this is known as charge-exchange injection, and allows an incoming beam to be combined with a proton beam that is already circulating in the synchrotron (or storage ring), this process is called multi-turn injection. This allows the beam current in the synchrotron (or storage ring) to build up to much higher levels than single turn proton injection [36].

Some cyclotrons use the same principle to facilitate accelerated ions' extraction. Negative ions circling through the cyclotrons have their electrons stripped for accelerated particle ejection from their circular path.

In a tandem accelerator the same electrostatic structure is used to accelerate a particle twice, first as a negative ion, then as a proton [1]. Due to the very high voltages required, tandem accelerators are only viable for beam energies of a few MeV.

Accelerator ion sources are characterised by their current output, pulse width and repetition rate (duty factor). Lifetime and emittance are also key quantities which determine a source's suitability for a particular accelerator. Beam shaping and co-extracted electrons are handled by an extraction system normally consisting of various electrodes with circular or slit apertures. Plasma volumes range from the size of a fingertip to a tennis ball depending on the technology employed.

Recent years have seen a move toward RF-driven inductively coupled volume sources following the success of the SNS source, in current output and reliability. Other technologies include magnetron, Penning, and surface

converter sources. Details including the advantages and disadvantages of each, and the widely used caesium enhancement may be found in [1,2].

China Spallation Neutron Source

For operations a penning source based on the ISIS H^- source is used. A RF driven external antenna, shown in Figure 3, is in development. Specifications of the two sources are in Table 7.

An ECR ion source is applied as a proton source for a linear accelerator on Boron Neutron Capture Cancer Therapy (BNCT) facility. Protons are accelerated up to 3.0MeV by RFQ and bombard the Li target.

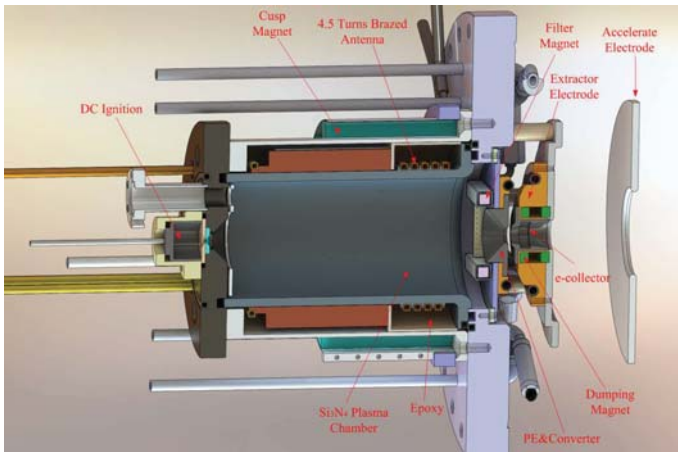

FIGURE 6. The RF source currently in commissioning at CSNS

TABLE 7. A comparison of the existing operational source and the external antenna RF source currently in commissioning

	Penning H^- ion source	**RF-External Antenna**
Status	Operation	Commissioning
Max Current	Up to 40mA	22mA-Uncesiated
Rep. Rate	25Hz	25Hz
Pul. Width	500us	Up to 1000us
Cesium Use	Cesiated	Uncesiated/Cesiated
Life time	4 weeks	>1 months

Fermilab

A magnetron H^- source feeds a magnetic LEBT, RFQ, MEBT, and DTL which accelerates the ions to 400 MeV. Electrons are stripped off at injection into a Booster ring which accelerates the remaining protons to 8 GeV prior to injection into the Main Injector for their final energy of 120 GeV. Protons are used for a wide range experiments ranging from fixed-target to neutrino production.

The operational source is a cesiated magnetron, with ions directly extracted at 35 keV, shown in Figures 4 and 5 below. It pulses at 15 Hz continuously for at least 9 months a year. High extraction voltage and low arc current have made for a long lifetime reliable source. The developmental PIXIE- D-Pace CW ion source produces 10 mA of H^- ions which are extracted at 30 kV into a magnetic LEBT and RFQ. This is a prototype front end for the future PIPII accelerator at FNAL. Table 8 compares the two sources.

A duoplasmatron proton source will produce 15 mA of H+ extracted at 30 kV for IOTA, a small R&D accelerator.

Further information can be found in references [37-40].

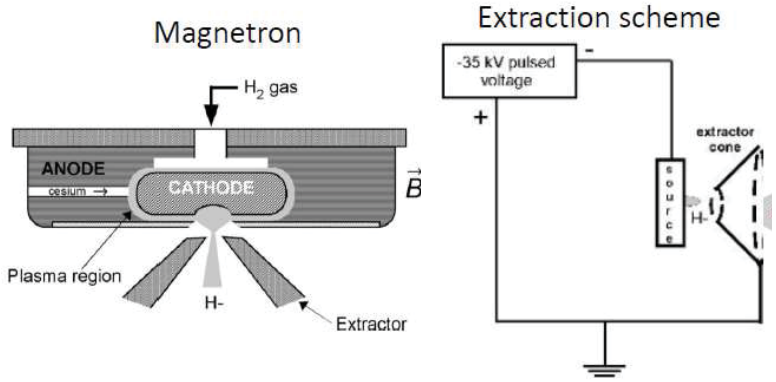

(a) (b)

FIGURE 7. (a) A diagram of the Fermilab magnetron (b) A simple diagram of the extraction scheme

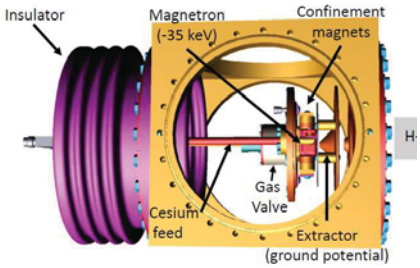

FIGURE 8. A model of the Fermilab magnetron

TABLE 8. A comparison of the sources used at Fermilab

Operational	PIXIE PIPII	IOTA/FAST
Magnetron	D-Pace Volume-Cusp	Duoplasmatron
60 mA (H^-)	10 mA (H^-)	100mA-Protons
200 us	DC	1.77 us
35 keV	30 keV	30 keV
15 Hz	CW	Single Turn

ISIS Neutron and Muon Source

An H^- ion source feeds a magnetic LEBT, RFQ, and DTL, for charge exchange injection into a rapid cycling synchrotron. Beam is accelerated to 800 MeV and directed onto tungsten and graphite targets to produce neutrons and muons for materials studies.

The operational Source is a caesiated Penning source, ions are extracted into 90° dipole with cooling to trap Cs, in Figure 6 below. VESPA is an experimental source, similar to the operational source without a dipole, developed to facilitate diagnoses, characterise the plasma, and experiment with performance. In order to experiment with higher currents and duty factors the 2X Scaled Source was developed. Again, similar to the operational source without dipole, but plasma chamber and aperture dimensions each doubled to ease thermal load on electrodes. Potential for use on FETS at RAL. Currently in development is the RF Source, and external antenna, 2MHz, uncaesiated source being designed and built to replace operational source, offering lifetime and reliability improvement. The design is largely based on CERN Linac4 and SNS. All the sources are compared in Table 9.

General introductory ion source texts can be found in Ref. [41], details about the operational source and VESPA are in [42], on the 2X source in [43,44], and the introduction to the RF project in [45].

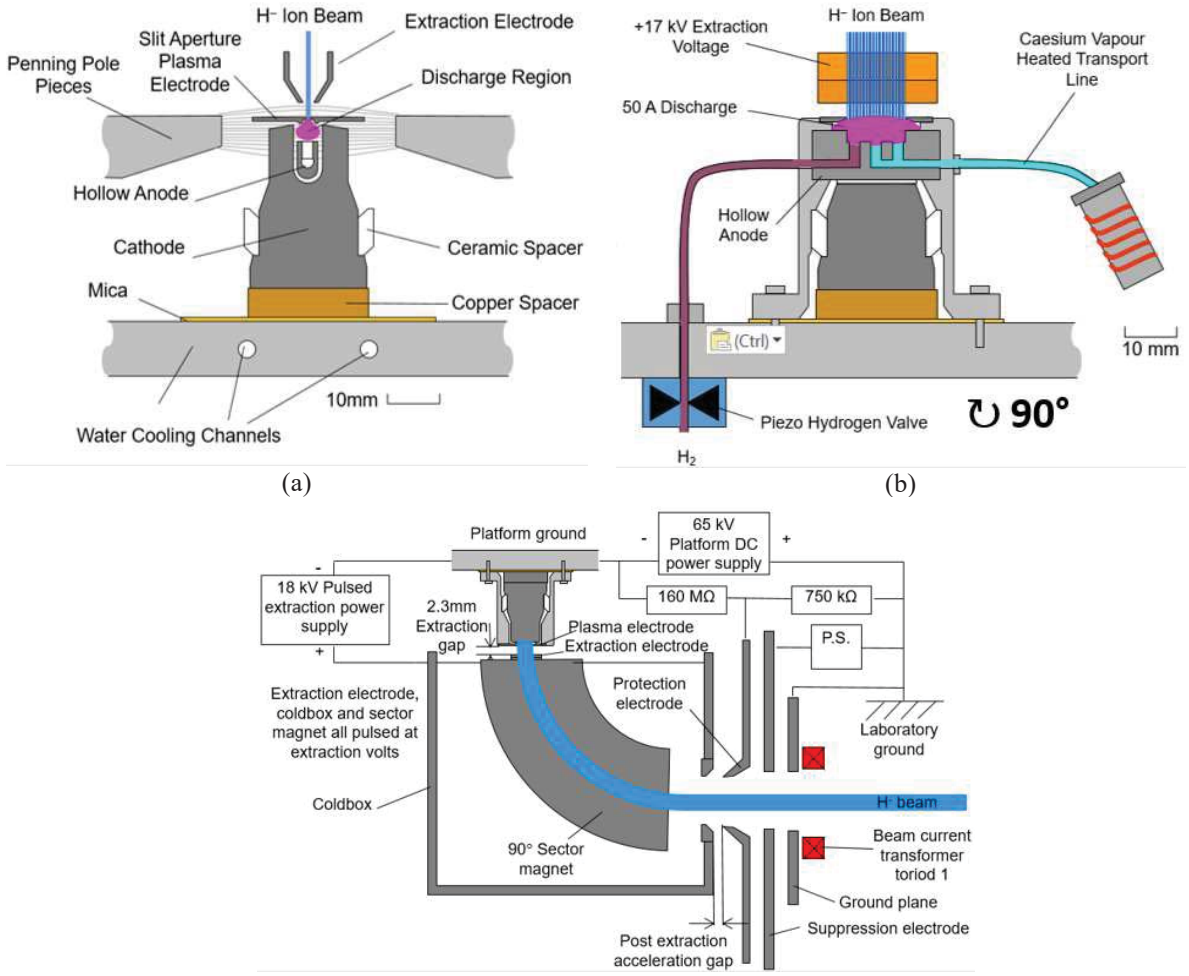

FIGURE 9. (a) and (b) diagram of the penning source design used for the operational source, VESPA, and 2X Source at ISIS, rotated 90 deg relative to each other. (c) A diagram of the extraction system and dipole used for the operational source.

TABLE 9. A comparison of the ion sources used for operations, experiments, and in development at ISIS

Operational	**VESPA**	**2X Scaled**	**RF Source**
Penning	Penning	Penning	Ext. Ant. RF
Operational	Experimental	Experimental	In development
55 mA	Up to 100 mA	75/150 mA	30mA
250 μs	Up to 1.2 ms	800/2000 μs	250 μs
Caesiated	Caesiated	Caesiated	Uncaesiated
All produce H^-, repetition rate 50 Hz			

Japan Proton Accelerator Research Complex (J-PARC)

J-PARC consists of a high-intensity proton accelerator and the experimental facilities that utilize the proton beam. The J-PARC accelerator consists of a linear accelerator (Linac), a Rapid Cycling Synchrotron (RCS) and a Main synchrotron Ring (MR). Figure 7 highlights key components of the complex. The proton beams accelerated at the RCS are delivered to the Materials and Life Science Experimental Facility (MLF) and injected into the MR. After the proton beams accelerated at the MR, they are delivered to the Neutron Production Facility (NU) or to the Hadron beam Facility (HD).

H^- ions are produced by an RF driven internal antenna source. Figure 8 shows a model of it and labels the key components. The inner volume of the plasma chamber is 100 mm in diameter and 120 mm in length. The H_2 plasmas is confined by an 18-pole cusp magnetic field. The aperture of the PE is 9 mm in diameter. Figure 9 shows the impressive operational time of various runs, and Table 10 contains the specifications of the JPARC source.

Linac

- H^- beam acceleration
- Beam energy : 400 MeV
- Beam current:
  - 50 mA for user operation
  - 60 mA for beam study (peak current at Linac exit)
- Pulse length : < 0.5 ms
- Repetition: 25 Hz

Rapid Cycling Synchrotron (RCS)

- Charge-exchange injection $H^- \rightarrow H^+$
- Beam energy: 3 GeV
- Injection into MR
- Delivery to MLF
- Beam supply to MLF with the beam power of 600 kW (in 2020)

Main Ring (MR)

- Beam energy :30 GeV
- Beam power
  - 500 kW (in 2020) to NU
  - 50 kW (in 2020) to HD

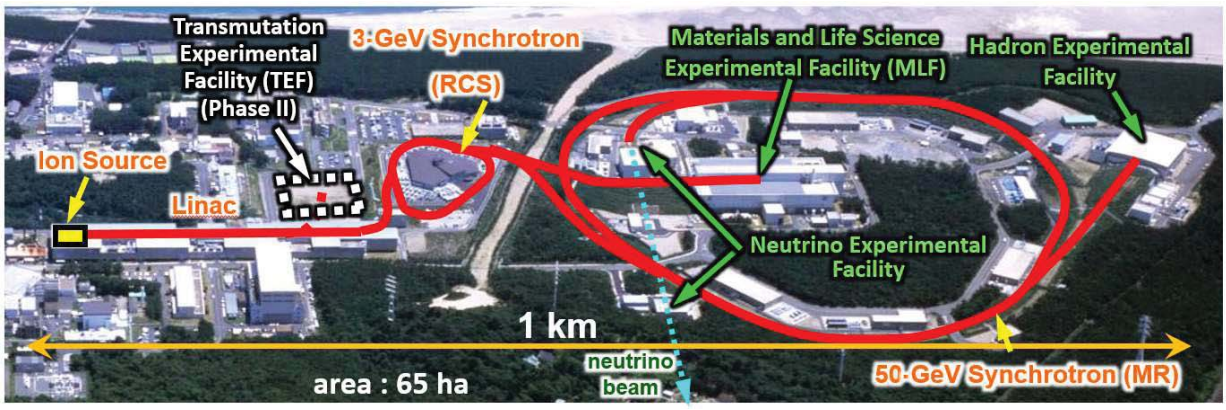

FIGURE 10. A diagram of J-PARC with key facilities and accelerator features labelled.

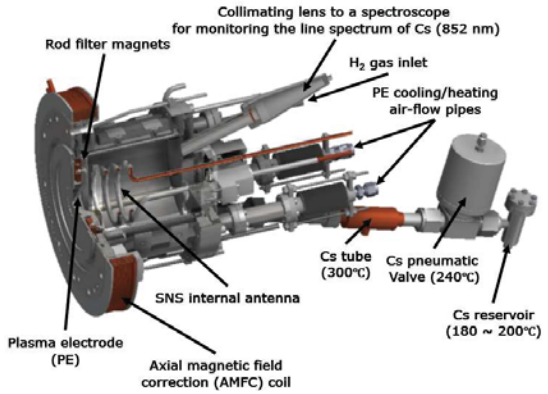

FIGURE 11. The J-PARC ion source with key features labelled

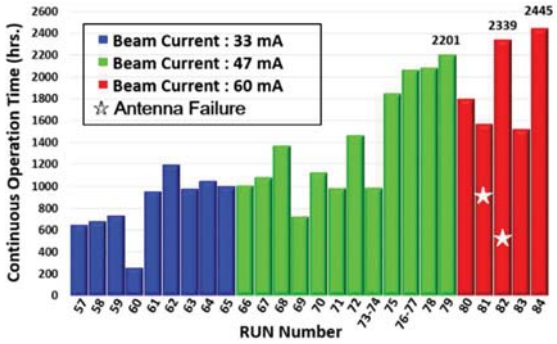

FIGURE 12. A plot of continuous operation times of recent runs, showing an increasing trend.

TABLE 10. Specifications of the J-PARC RF ion source

Specifications	
Discharge type	Internal antenna RF discharge
Repetition rate	25 Hz
RF frequency	30 MHz (cw, ~ 50 W) 2 MHz (0.8 ms pulsed, ~ 35 kW)
H_2 gas flow rate	21 sccm
Cs consumption	0.28 g in 1,567 hrs (in 2019)
Beam energy	50 keV
Extracted H^- beam current	60 mA (for user operation) 72 mA (for accelerator beam study)

Los Alamos Neutron Science Center (LANSCE)

A accelerator facility producing neutrons and protons, for isotope production, neutron scattering, and radiography. A linac accelerates H^- to 800 MeV or H+ to 100 MeV, before particles are directed onto the relevant target. H^- beam has 80 kV pre-extraction, then is accelerated to 750 kV using a Cockroft-Walton dome. Ions are produced at 120 Hz, in 833 us pulses of 14-16 mA by a multi-cusp caesiated surface conversion source, shown in a photo in Figure 13, and in a diagram in Figure 14. The converter surface is concave so ions produced on it are focused towards extraction. Each source lasts 4-5 weeks

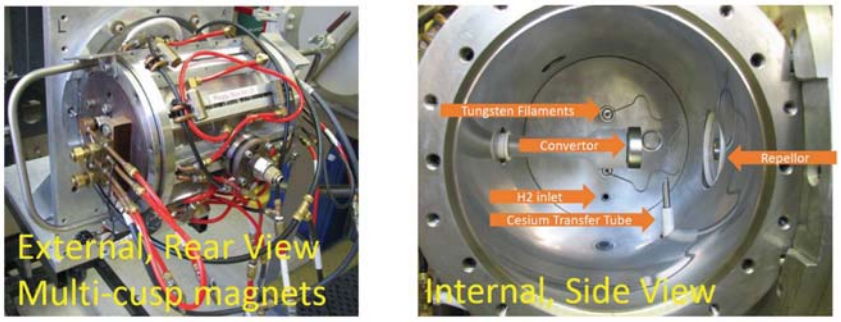

FIGURE 13. The LANSCE ion source viewed from behind, and on the inside. The concave convertor focusses ions for extraction.

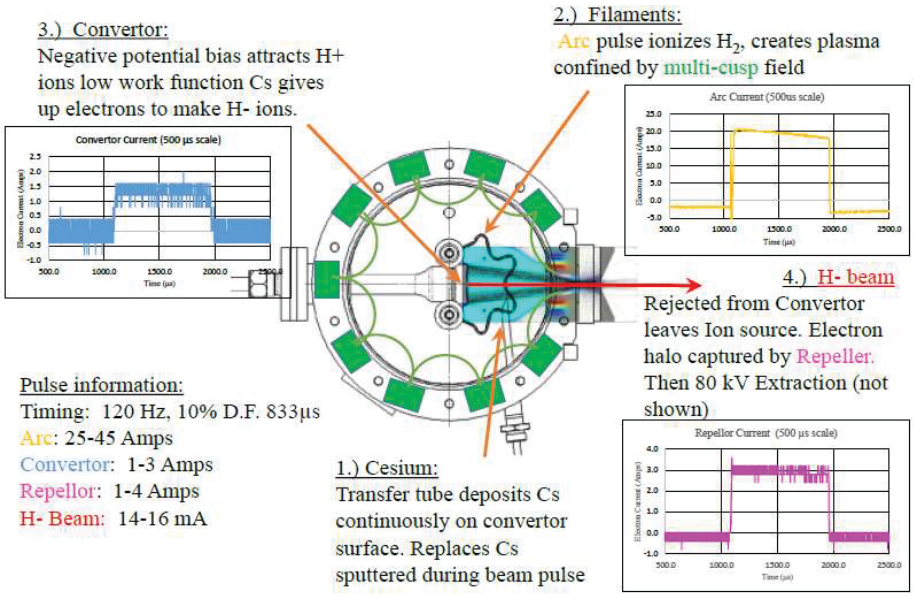

FIGURE 14. A diagram of the LANSCE ion source is labelled with the steps in ion production.

US Spallation Neutron Source

The Spallation Neutron Source (SNS) is the highest power pulsed neutron source currently operating worldwide and typically supports ~1000 users per year. The SNS accelerator system is sequentially comprised of an ion source, an electrostatic Low Energy Beam Transport system (LEBT), shown in Figure 15, a 2.5 MeV Radio Frequency Quadrupole accelerator (RFQ), a series of higher-energy linear accelerators producing a 1 GeV beam injecting a proton accumulator ring which subsequently directs beam onto a liquid Hg target producing neutrons. The ion source produces pulses of H^- ions with a current of 50-60 mA, pulse length of ~1 ms and repetition rate of 60 Hz. A LEBT chopping system divides the 1 ms pulse into ~1000 mini pulses for beam stacking into the ring and a fast kicker magnet then directs the stacked beam (~35 A at 1 GeV, ~1 us in duration) onto the Hg target at 60 Hz. Currently the SNS operates at 1.4 MW of proton beam power on target with plans to eventually reach 2.8 MW to simultaneously support a second target station. Approximately 35 and 46 mA, measured at the exit of the RFQ, are needed to achieve these target power levels, respectively.

The Cs-enhanced, RF-driven, multicusp ion sources employed at the SNS deliver 50-60 mA of H^- current (pulse width: 1ms at a repetition rate of 60Hz) through an electrostatic LEBT with a normalized emittance of < 0.3 π mm mrad. The source can operate for periods up to 4 months without maintenance. The ion source plasma is confined by a multicusp magnet field created by a total of 20 rare earth magnets lining the cylindrical chamber wall (φ=10 cm, l=10 cm) and 4 magnets lining the back plate. RF power (2 MHz, 50-60 kW) is applied to a porcelain coated Cu antenna coiled to 2 1/2 turns and is immersed within the plasma chamber. A magnetic dipole (200-300 Gauss) filter separates the main plasma from a smaller H^- production region where low-energy electrons facilitate the production of large amounts of negative ions. An air heated/cooled collar surrounding this H^- production volume dispenses small quantities of Cs to enhance H production. A mixture of Cs2CrO4 with Zr and Al is heated to release mg quantities of Cs. The back plate of the source which holds the antenna can be separated from the rest of the ion source to allow ease of maintenance. Once the negative ions are extracted a 1500-1700 G transverse magnetic field dumps the co-extracted electron beam on a dedicated dumping electrode maintained with a ~6 kV positive bias with respect to the extraction aperture. The SNS facility maintains 3 production internal antenna sources, 3 research-type internal antenna sources and 3 external antenna sources based on an AlN plasma chamber, a model of which is shown in Figure 16. More information can be found in references [46-51].

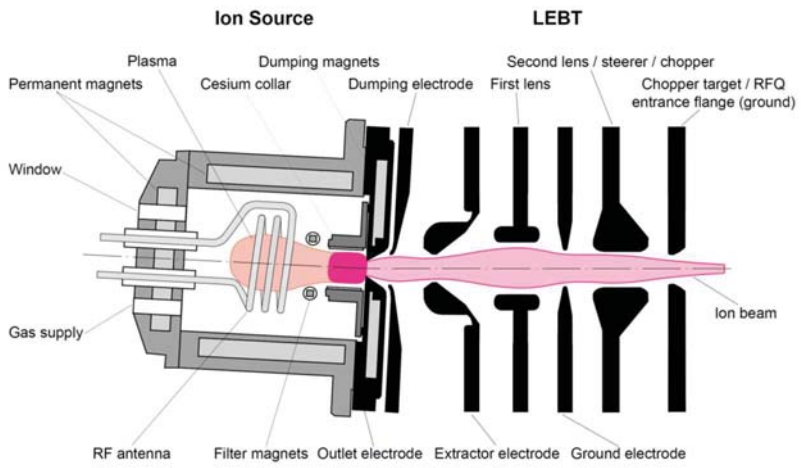

FIGURE 15. A diagram of the internal antenna RF source, and electrostatic LEBT used operationally at SNS

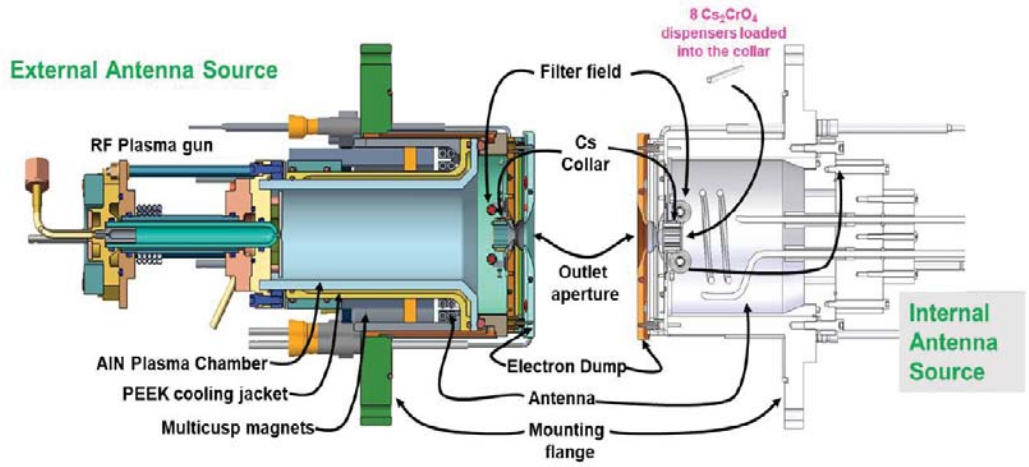

FIGURE 16. Diagram of external antenna source in comparison with internal antenna source used at SNS

ACKNOWLEDGEMENTS

The lead/corresponding author would like to thank the proceedings editors for their assistance in the production of this manuscript.

REFERENCES

1. D. Faircloth and S. Lawrie, New J. Phys. **20**, 025007 (2018).
2. M. Bacal and M.Wada. App. Phys. Rev. **2**, 021305. (2015)
3. U. Fantz and J. Lettry, New J. Phys. **20**, 060201 (2018)
4. Y. Ikeda et al, Nucl. Fusion **46**, S211 (2006).
5. M. Hanada et al, AIP Conf. Proc. **1390**, 536 (2011).
6. Y. Takeiri et al, Nucl. Fusion **46**, S199 (2006).
7. H. Nakano et al., AIP Conf. Proc. **1390**, 359 (2011).
8. E. Sartori et al., AIP Conf. Proc. **2011**, 080003 (2018).

9. Y. Haba, K. Nagaoka, K. Tsumori, M. Kisaki, H. Nakano, K. Ikeda, M. Osakabe, New J. Phys. **22** 023017 (2020).
10. A. Hurlbatt, N. den Harder, D. Wünderlich, and U. Fantz, Plasma Phys. Control. Fusion **61**, 105012 (2019).
11. K. Tsumori *et al*., AIP Conf. Proc. **763**, 35 (2004), K. Tsumori et al., Rev. Sci. Instrum. **79**, 02C107 (2008).
12. K. Tsumori *et al*., Fusion Sci. Tech. **58**, 489 (2010).
13. Y. Takeiri *et al*., AIP Conf. Proc. **1655**, 060004 (2015).
14. www.iter.org
15. R. Hemsworth, D. Boilson, P. Blatchford, M. Dalla Palma, G. Chitarin, H.P.L. de Esch, F. Geli, M. Dremel, J. Graceffa, D. Marcuzzi, G. Serianni, D. Shah, M. Singh, M. Urbani, P. Zaccaria, P, New J. Phys. **19**, 025005 (2017).
16. A.Chakraborty, C. Rotti, M. Bandyopadhyay, M. J. Singh, R.G. Nair, S. Shah, U. K. Baruah, R. Hemsworth, and B. Schunke, IEEE Trans. Plasma Sci. **38**, 248 (2010).
17. A. Kojima et al, Fusion Eng. Des. **123**, 236 (2017).
18. E. Speth, H.D. Falter, P. Franzen, U. Fantz, M. Bandyopadhyay, S. Christ, A. Encheva, M. Fröschle, D. Holtum, B. Heinemann, W. Kraus, A. Lorenz, C. Martens, P. McNeely, S. Obermayer, R. Riedl, R. Süss, A. Tanga, R. Wilhelm, and D. Wünderlich, Nucl. Fusion **46**, S220 (2006).
19. B. Heinemann, U. Fantz, W. Kraus, L. Schiesko, C. Wimmer, D. Wünderlich, F. Bonomo, M. Fröschle, R. Nocentini, and R. Riedl, New J. Phys. **19**, 015001 (2017).
20. D. Wünderlich, R. Riedl, F. Bonomo, I. Mario, U. Fantz, B. Heinemann, and W. Kraus, Nucl. Fusion **59**, 084001 (2019).
21. U. Fantz, F. Bonomo, M. Fröschle, B. Heinemann, A. Hurlbatt, W. Kraus, L. Schiesko, R. Nocentini, R. Riedl, and C. Wimmer, Fusion Eng. Des. **146**, 212 (2019).
22. D. Wünderlich, S. Mochalskyy, I.M. Montellano, and A. Revel, Review of Scientific Instruments **89**, 052001 (2018).
23. D. Wünderlich, M. Giacomin, R. Ritz, and U. Fantz, Journal of Quantitative Spectroscopy and Radiative Transfer **240**, 106695 (2020).
24. M. Kisaki, H. Nakano, K. Tsumori, K. Ikeda, S. Masaki, Y. Haba, Y. Fujiwara, K. Nagaoka, M. Osakabe, Rev. Sci. Instrum. 91 023503 (2020).
25. R. Friedl, Review of Scientific Instruments **87**, 043901 (2016).
26. S. Cristofaro, R. Friedl, and U. Fantz, Plasma Res. Express **2**, 035009 (2020).
27. U. Kurutz, R. Friedl, and U. Fantz, Plasma Phys. Control. Fusion **59**, 075008 (2017).
28. R. Friedl, S. Cristofaro, and U. Fantz, AIP Conf. Proc. **2011**, 050009 (2018).
29. D. Rauner, S. Briefi, and U. Fantz, Plasma Sources Sci. Technol. **26**, 095004 (2017).
30. D. Rauner, S. Briefi, and U. Fantz, Plasma Sources Sci. Technol. **28**, 095011 (2019).
31. R. Friedl, F. Merk, C. Hopf, and U. Fantz, AIP Conf. Proc. **2011**, 060006 (2018).
32. A. Heiler, R. Friedl, and U. Fantz, Journal of Applied Physics **127**, 113302 (2020).
33. J. Zacks, *et al*, AIP Conf. Proc. **1869**, 030047 (2017).
34. Yu. Belchenko, et al. Rev Sci Inst. **87**, 02B316. (2016).
35. M. Bacal and M.Wada. Plasma Sources Sci Tech. **29** 033001 (2020).
36. Dudnikov V. arXiv:180806002 [physics] (2018)
37. D.S. Bollinger, Review of Scientific Instruments **85**, 02B121 (2013).
38. D.S. Bollinger, P.R. Karns, and C. Tan, IEEE Transactions on Plasma Science **43**, 4110 (2015).
39. D.S. Bollinger, J. Lackey, J. Larson, and K. Triplett, Review of Scientific Instruments **87**, 02B902 (2015).
40. A. Sosa, D.S. Bollinger, P.R. Karns, and C.Y. Tan, AIP Conference Proceedings **2011**, 050001 (2018).
41. D. Faircloth, ArXiv:1302.3745 [Physics] (2013).
42. S.R. Lawrie, "Understanding the Plasma and Improving Extraction of the ISIS Penning H− Ion Source" Ph.D. Thesis, University of Oxford, 2017
43. D.C. Faircloth, S.R. Lawrie, J. Sherman, P. Wise, M.O. Whitehead, T. Wood, and T. Sarmento, in (Geneva, Switzerland, 2018), p. 050028.
44. D.C. Faircloth, S.R. Lawrie, O. Tarvainen, T. Sarmento, M.O. Whitehead, J. Macgregor, R. Abel, and T. Wood, in (Novosibirsk, Russia, 2018), p. 050004.
45. O. Tarvainen, S. Lawrie, D. Faircloth, R. Abel, T.M. Sarmento, J. Macgregor, M. Whitehead, T. Wood, J. Lettry, D. Noll, J.-B. Lallement, J. Angot, P. Sole, and T. Thuillier, in (Novosibirsk, Russia, 2018), p. 050005.
46. R. Keller, D. Cheng, R. DiGennaro, R.A. Gough, J. Greer, K.N. Leung, A. Ratti, J. Reijonen, R.W. Thomae, T. Schenkel, J.W. Staples, R. Yourd, A. Aleksandrov, M.P. Stockli, and R.W. Welton, Review of Scientific Instruments **73**, 914 (2002).

47. M.P. Stockli, R.F. Welton, and B. Han, Review of Scientific Instruments **89**, 052202 (2018).
48. M.P. Stockli, B.X. Han, S.N. Murray, T.R. Pennisi, M. Santana, C.M. Stinson, and R.F. Welton, AIP Conference Proceedings **1869**, 030010 (2017).
49. B.X. Han, R.F. Welton, S.N. Murray, T.R. Pennisi, M. Santana, C.M. Stinson, and M.P. Stockli, AIP Conference Proceedings **1869**, 030014 (2017).
50. R.F. Welton, B.X. Han, M.P. Stockli, S.N. Murray, T.R. Pennisi, C. Stinson, W. Barnett, A. Aleksandrov, M. Piller, R. Saethre, Y. Kang, and A. Zhukov, Review of Scientific Instruments **91**, 013334 (2020).
51. R.F. Welton, M.P. Stockli, Y. Kang, M. Janney, R. Keller, R.W. Thomae, T. Schenkel, and S. Shukla, Review of Scientific Instruments **73**, 1008 (2002).